

Depth-Dependent Sensitivity Correction

The sensitivity of the positron detector decreases as the distance between the detector and the layer of the medium increases because positrons interact before they reach the detector. The depth-dependent sensitivity profile of the TimePix chip was calibrated by a depth-dependent correction factor, which is estimated on the basis of Monte Carlo simulations using Geant4, a tool kit modeling the physical processes of particles passing through matter (1). The simulation of the positron measurement using the TimePix chip was verified in previous studies (2,3). As Supplemental Figure 1 displays, a surface source emitting ^{18}F positrons arbitrarily from a box region ($5 \times 5 \text{ cm}^2$) was placed on top of a $180\text{-}\mu\text{m}$ -thick plastic layer, a $6\text{-}\mu\text{m}$ -thick Mylar layer, and a $20\text{-}\mu\text{m}$ -thick air layer. The energy of the emitted positrons followed the theoretic ^{18}F positron energy spectrum (maximum energy, 633 keV). Layers of water $20 \mu\text{m}$ thick were then inserted one after another between the surface source and the plastic layer. The depth-dependent sensitivity profile was derived as follows:

$$f(x) = -0.00104x + 0.4732 \text{ (cps/Bq)},$$

where x denotes the thickness of water between the source and the plastic layer. In the microfluidic study, the medium is diluted with radioactivity. Given an investigated region of area A and a radioactivity concentration of ρ in the medium, the counted events y of the positron detector are a function of the thickness of the medium l :

$$y(l) = \int_0^l f(x) A dx \rho = -0.00052 A \rho l^2 + 0.4732 A \rho l.$$

The correction factor α for a thicker layer (L_2) to a thinner layer (L_1) is as follows:

$$\alpha = \frac{L_2}{L_1} / \left(\frac{y(L_2)}{y(L_1)} \right) = \frac{(-0.00052 L_1^2 + 0.4732 L_1) L_2}{(-0.00052 L_2^2 + 0.4732 L_2) L_1}.$$

In this study, the average diameter of the cell is $45.9 \mu\text{m}$, and we assume the thickness of the cell to be $22.95 \mu\text{m}$. Thus, the correction factor α applied in this study is 1.74.

Influence of Sensitivity

The processing of data in this study does not consider the absolute radioactivity concentration. Instead, it estimates uptake values and kinetic parameters using the event density based on measurements of positron events captured in the positron detector. Assuming that the sensitivity of the detector to the cell layer is θ and the medium events have already been corrected for depth-dependent sensitivity to the cell layer (Supplemental Fig. 1). For delay and dispersion correction, the measured medium event density in the cell chamber without cells is $\beta_{cm}(t)$ and the measured medium events in the medium chamber is $\beta_m(t)$:

$$\beta_{cm}(t) = \beta_m(t - \Delta T) * \frac{1}{\tau} e^{-t/\tau}.$$

The absolute activity concentration $C_m(t)$ in the medium chamber is

$$C_m(t) = \frac{\beta_m(t)}{\theta}.$$

The absolute activity concentration of the medium in the cell chamber $C_{cm}(t)$ is

$$C_{cm}(t) = \frac{\beta_{cm}(t)}{\theta} = \frac{\beta_m(t - \Delta T) * \frac{1}{\tau} e^{-t/\tau}}{\theta}.$$

As θ is constant during the same measurement, we could derive

$$C_{cm}(t) = C_m(t - \Delta T) * \frac{1}{\tau} e^{-t/\tau}.$$

Thus, the delay and dispersion corrections are not influenced by the sensitivity and can be

applied to event density.

Given the event density of cells in cell chamber $\beta_{cc}(t)$, the normalized uptake is

$$\omega(t) = \frac{\beta_{cc}(t)}{\beta_{cm}(t)} = \frac{\beta_{cc}(t)/\theta}{\beta_{cm}(t)/\theta} = \frac{C_{cc}(t)}{C_{cm}(t)},$$

where $C_{cc}(t)$ is the absolute activity concentration of cells in the cell chamber. It is equivalent to the normalized uptake using absolute activity concentration.

Further, for the cellular pharmacokinetic modeling, the modeling equation can be derived as follows (4):

$$\begin{aligned}\beta_{cc}(t) &= \beta_{in}(t) + \beta_{ph}(t) \\ &= a_1 e^{-b_1 t} * \beta_{cm}(t) + a_2 e^{-b_2 t} * \beta_{cm}(t)\end{aligned}$$

where

$$a_1 = \frac{k_1(b_1 - k_3 - k_4)}{\Delta}$$

$$a_2 = \frac{k_1(b_2 - k_3 - k_4)}{-\Delta}$$

$$b_1 = \frac{k_2 + k_3 + k_4 + \Delta}{2}$$

$$b_2 = \frac{k_2 + k_3 + k_4 - \Delta}{2}$$

$$\Delta = \sqrt{(k_2 + k_3 + k_4)^2 - 4k_2k_4}$$

As the absolute activity concentration of cells in cell chamber $C_{cc}(t)$ is

$$\begin{aligned}C_{cc}(t) &= \frac{\beta_{cc}(t)/\theta}{\theta} \\ &= \frac{a_1 e^{-b_1 t} * \beta_{cm}(t) + a_2 e^{-b_2 t} * \beta_{cm}(t)}{\theta}\end{aligned}$$

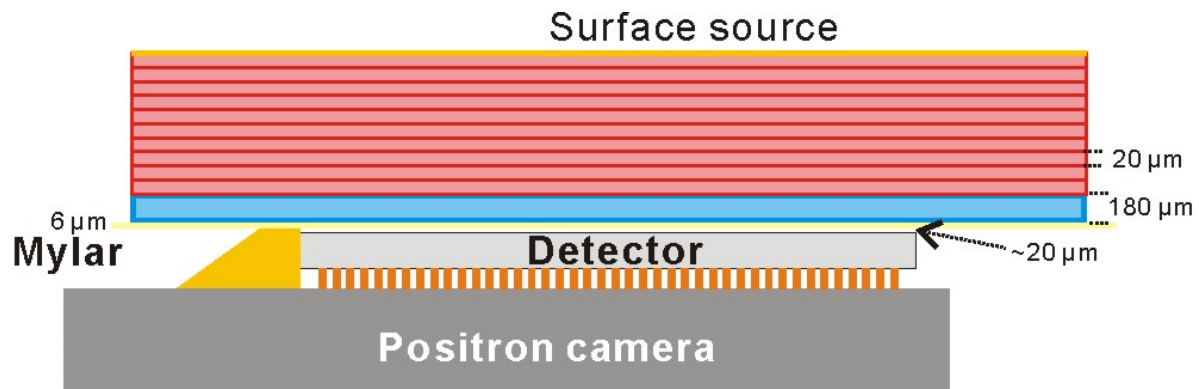
θ is constant, and $C_{cm}(t) = \beta_{cm}(t)/\theta$, we can derive

$$C_{cc}(t) = a_1 e^{-b_1 t} * C_{cm}(t) + a_2 e^{-b_2 t} * C_{cm}(t).$$

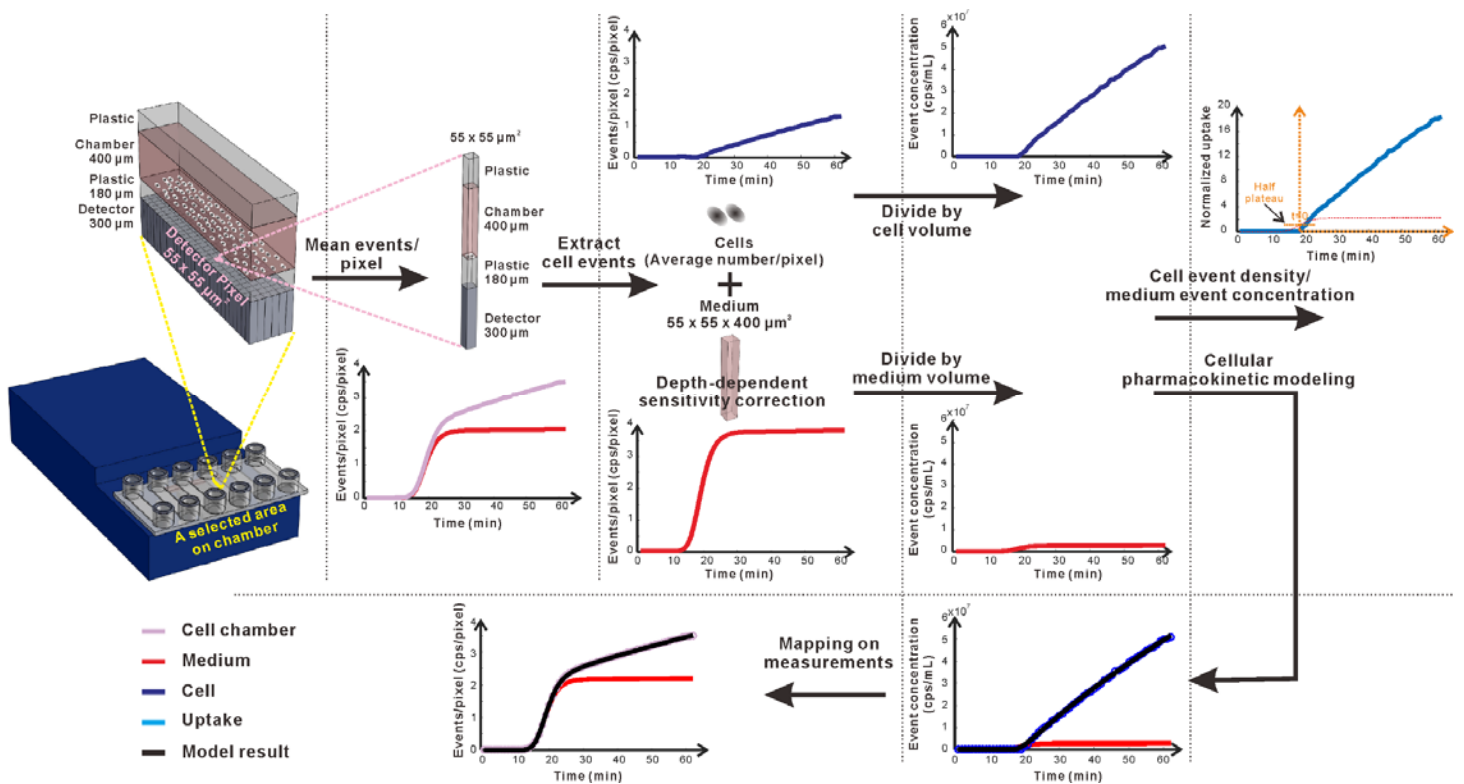
Use of event density is equivalent to use of absolute radioactivity concentration in the parameter estimation of cellular pharmacokinetic modeling.

References

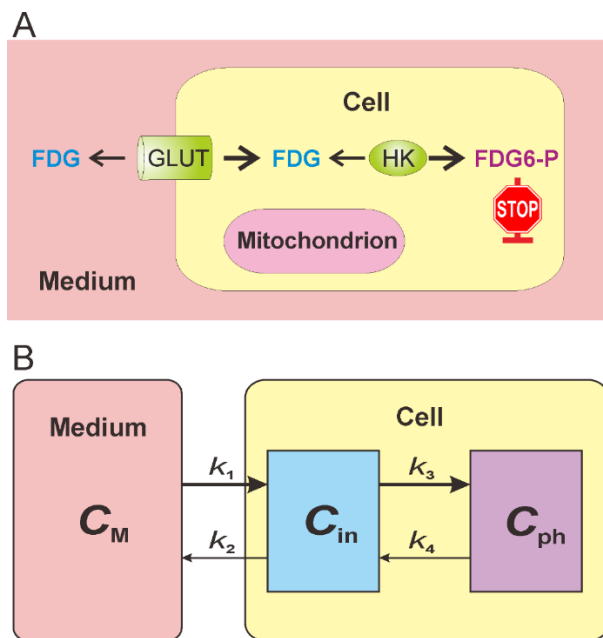
1. Allison J, Amako K, Apostolakis J, et al. Geant4 developments and applications. *IEEE Trans Nucl Sci.* 2006;53:270–53278.
2. Wang Q, Tous J, Liu Z, Ziegler SI, Shi K. Evaluation of Timepix silicon detector for the detection of ^{18}F positrons. *J Instrument.* 2014;9:C05067.
3. Wang Q, Liu Z, Ziegler SI, Shi K. Enhancing spatial resolution of F positron imaging with the Timepix detector by classification of primary fired pixels using support vector machine. *Phys Med Biol.* 2015;60:5261–5278.
4. Gunn RN, Gunn SR, Cunningham VJ. Positron emission tomography compartmental models. *J Cereb Blood Flow Metab.* 2001;21:635–652.



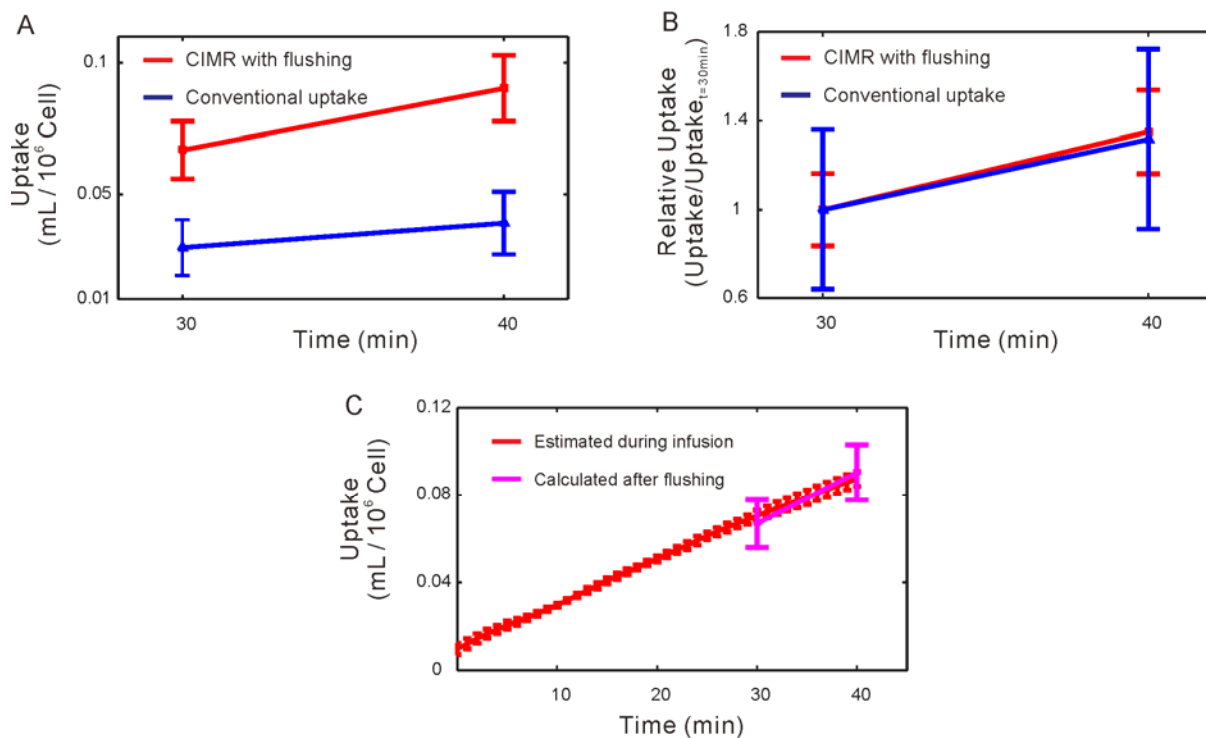
Supplemental Figure 1. Depth-dependent sensitivity correction.



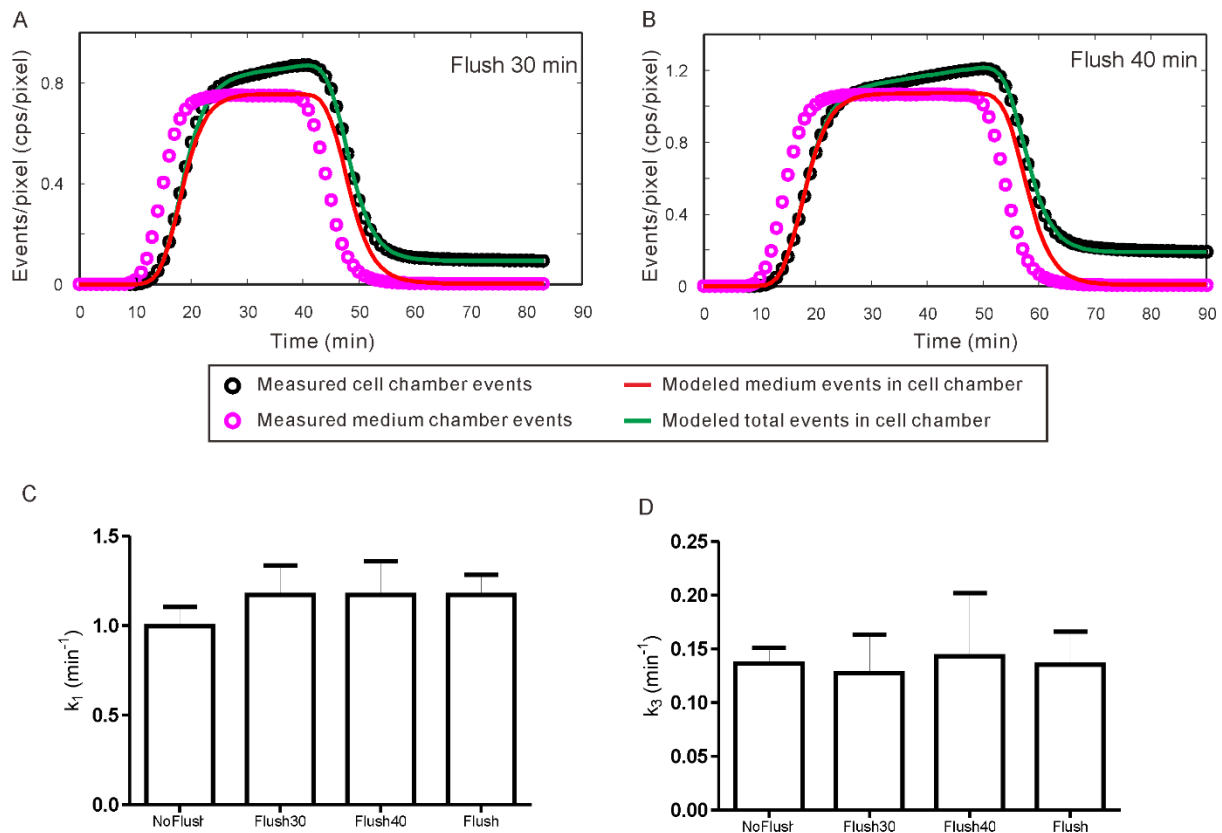
Supplemental Figure 2. Data processing procedure.



Supplemental Figure 3. Diagrams of (A) the FDG uptake procedure and (B) the corresponding cellular pharmacokinetic modeling.



Supplemental Figure 4. Comparison of uptake obtained on CIMR and on conventional uptake experiment using well counter: (A) comparison of estimated uptake between CIMR after flushing the tracer at 30 and 40 min and conventional ex-culture uptake ($n = 3$); (B) comparison of relative uptake of A by normalizing each uptake value to the mean values to 1; (C) comparison of two CIMR uptake values, the estimated real-time uptake value using continuous infusion profile, and the uptake value after flushing the tracer at 30 and 40 min.



Supplemental Figure 5. A test of CIMR using square function infusion profile: (A) an example measurement with flushing of tracer at 30 min after infusion and the corresponding curve fitting; (B) an example measurement with flushing of tracer at 40 min after infusion and the corresponding curve fitting; (C) comparison of the k_1 parameters using step function (NoFlush, $n = 6$), flushing at 30 min (Flush30, $n = 3$), and flushing at 40 min (Flush40, $n = 3$) and the summary of Flush30 and Flush40 (Flush, $n = 6$); (D) comparison of the k_3 parameters using step function (NoFlush, $n = 6$), flushing at 30 min (Flush30, $n = 3$), and flushing at 40 min (Flush40, $n = 3$) and the summary of Flush30 and Flush40 (Flush, $n = 6$).